CrossMark

Characterization, Distribution, and Source Analysis of Metals and Polycyclic Aromatic Hydrocarbons (PAHs) of Atmospheric Bulk Deposition in Shanghai, China

Jing Liang · Hailan Fang · Longhua Wu · Taolin Zhang · Xingxiang Wang

Abstract The bulk deposition of both PAHs and metals is a significant, mounting issue for the urban ecological environment. However, studies generally performed on these pollutants have focused on the regions surrounding a pollution source; thus, it most likely overestimated pollutants in the cities. Therefore, 72 atmospheric bulk deposition samples were collected from six sites located along a transect from the suburbs to the city center in Shanghai over a 1-year period (February 1, 2012 to January 31, 2013). The seasonal variation, spatial distribution, and sources of multiple metals (Al, Ti, V, Cr, Mn, Co, Ni, Cu, Zn, As, Cd, Pb, K, Na, and Mg) and 16 polycyclic aromatic hydrocarbon (PAH) compounds were determined. The results indicated that the annual average rate of dust deposition in Shanghai was $43,100 \pm 54,800$ mg/m^2/year. There were significant or high enrichments of Cu, Zn, Cd, and Pb, and higher depositional fluxes were observed for Zn, Pb, and Cd in the Huangpu district and for Cu in the Minhang district. The deposition fluxes of the PAHs exhibited the following order: urban fringe zone > city center > rural zone (background site). However, unlike in northern Chinese cities, the high-molecular-weight PAHs accounted for most of the PAHs. Furthermore, there were higher depositional fluxes of PAHs in March, July, and October. Overall, the factors influencing urban air quality may include construction, fossil fuel combustion, the abrasion of tires and brake linings (directly related to traffic), the corrosion of galvanized protection barriers, and increasing population density.

J. Liang · L. Wu · T. Zhang · X. Wang (✉)
Key Laboratory of Soil Environment and Pollution Remediation, Institute of Soil Science, Chinese Academy of Sciences, Nanjing 210008, People's Republic of China
e-mail: xxwang@issas.ac.cn

J. Liang · L. Wu · T. Zhang · X. Wang
University of Chinese Academy of Sciences, Beijing 100049, People's Republic of China

J. Liang · H. Fang
Shanghai Institute of Landscape Gardening, Shanghai 200232, People's Republic of China

1 Introduction

In China, the economy has developed rapidly in the last two decades, but pollution control measures have not kept in pace with the rapid economic growth (Davis and Guo, 2000) and air pollution have become a serious problem (Cao et al., 2011) and led to the frequent occurrence of hazy weather.

The atmosphere is a medium through which certain natural, anthropogenic, organic, and inorganic chemicals are transported, and wet and dry deposition are the most important processes that remove these chemicals from the atmosphere (Amodio et al., 2014). Numerous studies have shown that atmospheric deposition may transfer

atmospheric pollutants [dust, particulate matter containing heavy metals, polycyclic aromatic hydrocarbons (PAHs), dioxins, furans, sulfates, nitrates, etc.] to terrestrial and aquatic ecosystems (Azimi et al. 2003; Azimi et al. 2005; Cao et al. 2011; Wang et al. 2011; Shi et al., 2012; Yan et al. 2012; Gunawardena et al. 2013; Liu et al. 2013). Therefore, atmospheric deposition has currently garnered considerable attention from the scientific community and has become a specific research area in the environmental sciences.

Because of the well-known carcinogenic and mutagenic properties of PAHs (Lee et al. 1981; Williams 1990; Ravindra et al. 2008; Tobiszewski and Namiesnik 2012) and the high toxicity and liability of heavy metals (Golomb et al. 1997), an increasing number of research studies have commenced to determine the levels of PAHs (Liu et al. 2013; Wang et al. 2011; Yan et al. 2012) and heavy metals (Cao et al. 2011; Gunawardena et al. 2013; Shi et al. 2012) in atmospheric deposition. However, few studies have considered the simultaneous deposition of both atmospheric PAHs and heavy metals (Azimi et al. 2005). Moreover, the studies generally performed on these pollutants have focused on the regions surrounding a pollution source, where a limited number of people come into contact with the pollutants (Bari et al. 2014); thus, it most likely overestimated pollutants in the cities. Bari et al. (2014) showed that the metal and PAH deposition amounts at sampling sites greater than 45 km from an oil sands development were smaller than those at the sites within 20 km of the oil sands development. Therefore, the deposition amounts of the metals and PAHs decreased with distance from the emission sources. Sabin et al. (2006) also discovered that dry deposition fluxed and that the atmospheric concentrations of chromium, copper, lead, nickel, and zinc were highest at the site closest to the freeway and reduced to approximately urban background concentrations between 10 and 150 m downwind of the freeway. With the rapid expansion of urban development in China, there is obviously great interest in characterizing the magnitude and extent of metal and PAH deposition in the region. In urban areas, these pollutants have become a potential threat to human health and safety, and they have severely disturbed the natural geochemical cycling of ecosystems. Furthermore, metals and PAHs have a direct influence on public health because they can easily enter human bodies through routes such as dust ingestion, dermal contact, and breathing (Abrahams 2002; Liu et al. 2013).

Shanghai has the largest and the densest population of all cities in China and is similar to other major metropolitan cities in the world. Therefore, it is facing more pressure to provide better environmental protection for its citizens and to restore the existing environmental damage. Recently, however, with the development of environmental regulations and with investments in environmental management and pollution controls (e.g., relocating heavy industries from the urban centers to less-populated remote areas, converting coal-fired industrial boilers to cleaner fuels), directing the focus to only studies near pollution sources may overestimate the risks to public health in the city. Therefore, in this study, five districts (Huangpu, Luwan, Xuhui, Minhang, and Songjiang) and one reference site (background site) were selected along a spatial gradient from the city center to the suburbs to study the characteristics of dry and wet deposition.

The aims of the study were (1) to measure the bulk deposition and fluxes (dry deposition and wet deposition) of PAHs and metals in the different districts, (2) to investigate the spatial and seasonal variations of the bulk deposition fluxes of the PAHs and metals, and (3) to identify the possible sources of the PAHs and trace elements in bulk deposition.

2 Methodology

2.1 Sampling Strategies

Five districts in Shanghai (Huangpu, Luwan, Xuhui, Minhang, and Songjiang) were selected along a transect from the suburbs to the city center to determine the gradient of atmospheric deposition with respect to distance from the city center. The Huangpu and Luwan districts are enclosed by the inner traffic ring, and the Xuhui district is located between the inner and middle traffic rings; these three districts are characterized by very dense commercial and residential areas. The Minhang district is situated on the urban fringe between the middle and outer traffic rings and has highly dense industrial and moderately dense residential areas. The Songjiang district is located beyond the outer traffic rings and has low density residential areas. The population densities of each of the five districts were 34,625, 30,889, 19,817, 6,558 and 2,614 people per square kilometer, respectively (Shanghai Municipal Statistics Bureau, 2010). The sampling sites used in the study are

shown in Fig. 1. To identify the source of the PAHs and the metals, a reference site was established at the Shanghai Chenshan Botanical Garden (newly constructed in 2007), which is located in the Songjiang district, far from the city center.

All locations had relatively easy vehicle access and were situated in open areas without trees. The height of the sampling inlet was at least 3 m above ground to avoid sample contamination due to ground effects. Rectangular containers (height 0.4 m) with top surface areas of 0.35 m^2 were used to collect bulk deposition (Wang et al., 2011; Zhang et al., 2011), and the containers were all made of polytetrafluoroethylene (Teflon) to minimize their adsorption of PAHs (Tasdemir et al., 2007).

As a coastal city influenced by the Asian Monsoon, the prevailing wind in Shanghai is southeasterly (oceanic) in spring and summer and northwesterly in autumn and winter (Feng et al. 2013; Zhao et al., 2015). Bulk deposition samples were collected monthly using a bulk deposition sampler that operated from February 1, 2012 to January 31, 2013. A total of 72 samples were collected from the six sites. The design of the bulk samplers was based on the evaluation of similar equipment according to China's national standard (GB/T 15265-1994). Replicate sampling equipment ($n = 3$) was deployed at every site. Distilled water was added to the bulk deposition sampler before sampling, with the amount varying according to the season (generally
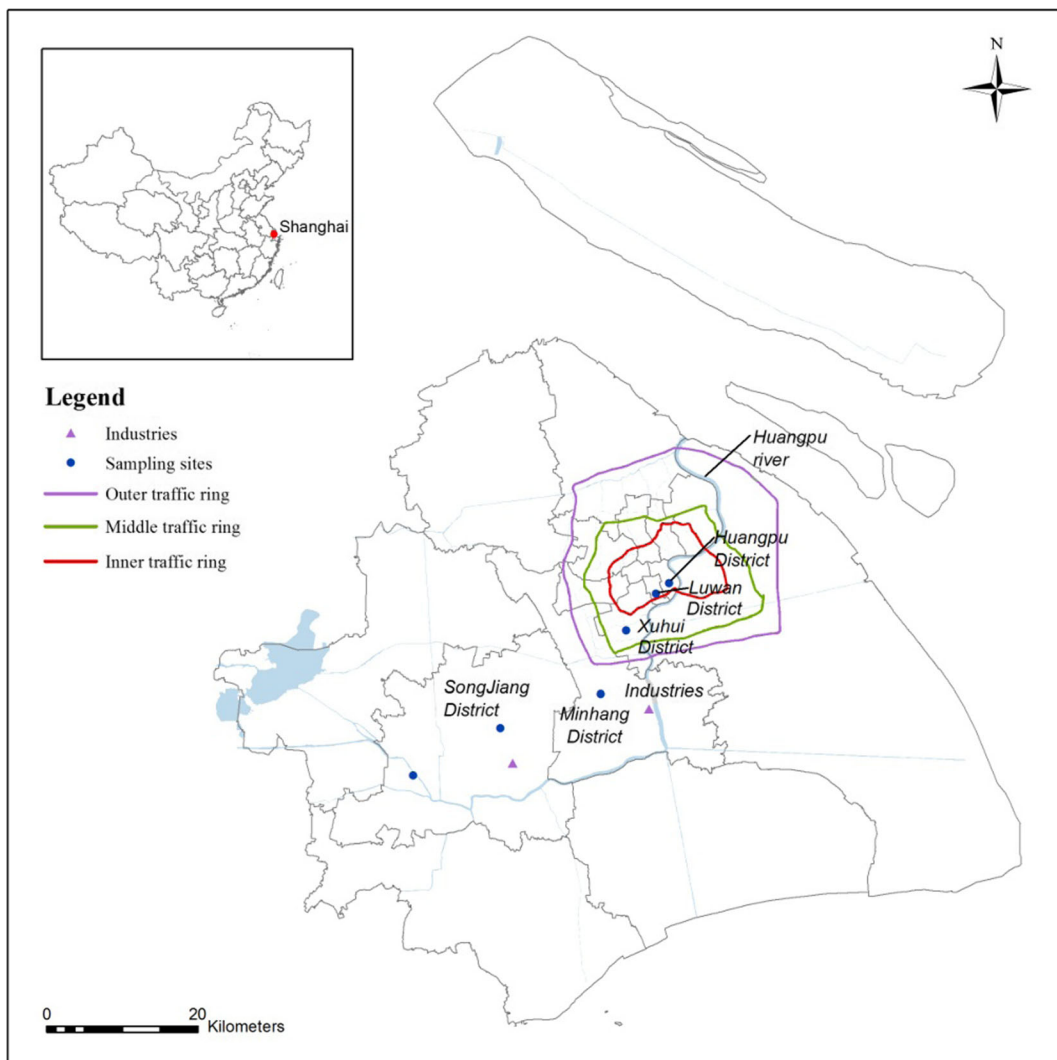
Fig. 1 Map of the sampling locations in Shanghai

50 mL in summer and winter and 100 mL in spring and fall). Approximately 60 mL of ethylene glycol was also added to each sampler to prevent the water from freezing in the winter and to reduce the effects of biodegradation.

At the end of every month, the bulk deposition samplers were capped, enclosed with black shell, and transported to the laboratory. Leaves and insects were removed using forceps before sample treatment. Samples were air-dried at ambient room temperature, collected by a clean brush, and ground to pass through a 100-μm sieve. The samples obtained were stored at 0–4 °C before analysis to prevent the volatilization of PAHs (Yan et al. 2012; Peng et al. 2012).

Additionally, prior to deployment in the field for deposition sampling, the samplers were soaked with 5 % nitric acid for at least 24 h and rinsed with double-distilled water (DDW) at least three times to ensure sampler cleanliness.

2.2 Sample Extraction and Determination

2.2.1 Validation of the Sampling Device

All settled atmospheric deposition samples were analyzed by direct weighing using an electronic analytical balance (Sartorius TE 612-L, Sartorius Stedim (Shanghai) Trading Co. Ltd, Zhangjiang, China) with ±0.01 g accuracy. The bulk deposition samples collected by the sampling equipment were weighed, and the reproducibility of parallel bulk sampling was less than 10 %. Moreover, a modified cleaning procedure was applied prior to sample collection based on the one employed by Foan et al. (2012) and Tasdemir et al. (2007). After being rinsed with organic solvents, the sampling devices were rinsed again with double-distilled water, and the contents of the inorganic elements and PAHs in the discharged water were then detected to validate the efficiency of cleaning procedure. The results showed that the concentrations of the detected contaminants were all below the detection limits, which indicated that no contamination by inorganic elements and PAHs occurred in the sampling device prior to sampling. The inorganic element and PAH contents for the brush and the collectors after collecting samples were also under the detection limits. Therefore, the loss of the inorganic elements and PAHs in the samples was low.

2.2.2 Analysis and Quality Control of Inorganic Elements

The composition of the inorganic elements in the samples was determined by inductively coupled plasma-mass spectrometry (ICP-MS; Perkin-Elmer Elan DRC-II). The metals measured were aluminum (Al), titanium (Ti), vanadium (V), chromium (Cr), manganese (Mn), cobalt (Co), nickel (Ni), copper (Cu), zinc (Zn), arsenic (As), cadmium (Cd), lead (Pb), potassium (K), sodium (Na), and magnesium (Mg).

Approximately 0.50 g of the deposition sample was placed in a polytetrafluoroethylene (PTFE) vessel. The samples were digested with concentrated nitric acid (HNO_3), hydrofluoric acid (HF), and perchloric acid ($HClO_4$) in a microwave oven. Sediment standards (GSS-6 and GSS-7), supplied by Chinese National Research Center for Certified Reference Materials, were used for quality assurance and quality control (QA/QC). The recovery values for all elements were between 88 and 112 %. Duplicate samples were analyzed to verify accuracy, and the standard deviation was within 5 %. Moreover, blank determinations were performed in triplicate throughout all experiments. To avoid contamination, the acid used for sample analysis was a guaranteed reagent, and all containers used were immersed in 10 % (v/v) HNO_3 before analysis.

2.2.3 Analysis and Quality Control of PAHs

The extraction and cleanup procedures were conducted according to the results of a previous study, as described below (Liang et al. 2011). A dust sample (0.50 g) was transferred into a Soxhlet extractor and was extracted for 24 h using 75 mL of an acetone and dichloromethane mixture (1:1, v:v) in a 65 °C water bath. Activated copper powder was added to remove sulfur from the extracts. The extract solutions were then concentrated in a rotary evaporator and cleaned up using a chromatographic column consisting of 10 g of neutral aluminum oxide, 5 g of activated silica gel, and 5 g of anhydrous sodium sulfate to minimize interference with non-target compounds. The column was subsequently eluted with 30 mL of n-hexane, 30 mL of an n-hexane and dichloromethane mixture (4:1, v:v), and 30 mL of another n-hexane and dichloromethane mixture (2:1, v:v). The eluent obtained was further cleaned up with sulfuric acid, distilled water, and anhydrous sodium sulfate to remove esters, residual acid, and water, respectively.

Finally, the solution was concentrated and the volume was fixed in a 5-mL-volumetric flask with dichloromethane (chromatographic grade) before analysis.

All solvents used in this experiment were pure or chromatographic grade. Quantitative analysis of the deposition samples was conducted by gas chromatography-mass spectrometry (GC/MS). The GC time–temperature profile was programmed as follows: heat to 60 °C, hold for 2 min, heat to 150 °C at 30 °C/min, hold for 1 min, and then heat to 300 °C at 6 °C/min, hold for 10 min. The transfer line temperature was 290 °C. High-purity helium was used as the carrier gas at a constant flow rate (1 mL/min) with the splitless injection. Mass detection was performed in the single ion monitoring (SIM) mode. The GC/MS was calibrated once a week.

The identification and quantification of the 16 PAHs was accomplished by matching their retention time with a mixture of PAH standards. The 16 PAHs were naphthalene (Nap), acenaphthylene (Any), acenaphthene (Ann), fluorene (Fle), phenanthrene (Phe), anthracene (Ant), fluoranthene (Flu), pyrene (Pyr), benzo(a)anthracene (Baa), chrysene (Chr), benzo(b)fluoranthene (Bbf), benzo(k)fluoranthene (Bkf), benzo(a)pyrene (Bap), indeno(1,2,3)pyrene (I1P), dibenz(a,h)anthracene (Daa), and benzo(g,h,i)perylene (Bgp).

Serial dilutions of the PAH standards (610/525/550 in methanol from Chem Service, USA) were analyzed to ensure the detection limit for the individual PAH compounds. The detection limit (LOD) ranged from 0.005 (Phe) to 0.1 mg/kg (Bgp). Two laboratory blanks were analyzed in addition to the samples, and the contents of the PAHs were corrected accordingly.

Furthermore, the recovery efficiencies were established by introducing a known concentration of the PAH standard into the control sample. The recovery efficiency of the compounds ranged from 70 % (Nap) to 104 % (BgP), with an average of 78 %. Three replicate samples were reanalyzed, and the variation in the PAH concentrations for these samples was less than 20 %.

2.3 Statistical Estimation

The deposition rate (DS) was calculated using the following equation: $DS = \frac{Ms}{A*D}$, where DS (mg/m^2/day) is the atmospheric deposition rate, Ms (mg) is the dry weight of the atmospheric deposition sample, A (m^2) is the area of the sampler, and D (day) is the number of days sampled in every month (Cao et al. 2011)

The enrichment factor (EF) value of an element, X, can be calculated by:

$$EF = \frac{\left[X \big/ R \right]_{Sample}}{\left[X \big/ R \right]_{Crust}},$$

where R is the reference element in the crustal material (i.e., Ti in this study), $[X/R]_{Sample}$ is the ratio of X to R in the deposition sample, and $[X/R]_{Crust}$ is the ratio of X to R in the crust. The concentrations of X and R in the crust were confirmed based on previously determined Chinese soil values (Chen et al. 1991).

The EF of an element in a sample is based on the standardization of the measured element against a reference. Generally, Si, Al, Fe, or Ti are used as reference elements (Martín et al. 2009). In this study, Ti was chosen as the reference element because it is a major crustal component and rarely influenced by human activity.

Numerous studies have indicated that five accumulation classes can be differentiated based on the EF: deficiency to minimal enrichment (EF <1 is recognized as no enrichment, while 1< EF <2 is recognized as minimal enrichment), moderate enrichment (2< EF <5), significant enrichment (5< EF <20), very high enrichment (20< EF <40), and extremely high enrichment (EF >40; Sutherland 2000).

To clearly represent the seasonal variation of elemental concentrations, the min–max normalization of deposition rates of all elements were calculated by:

$$x* = \frac{x - min}{max - min},$$

where $x*$ is a min–max normalized value, x is a raw score to be standardized for deposition rate of the element, min is the minimum of deposition rate of the element, and max is the maximum of deposition rate of the element.

The ratios of individual PAH species are frequently used as a diagnostic tool to determine the origin of the PAHs (Yunker et al. 2002; Wang et al. 2011; Yan et al. 2012). Generally, the Ant/Ant+Phe ratio within the three-ring PAHs, BaA/BaA+Chr within the four-ring PAHs, and IcdP/Icdp+BghiP within the six-ring PAHs have been used to distinguish between pyrogenic sources (e.g., coal burning, wood burning, and vehicular exhaust emissions) and petroleum origins. An Ant/Ant+Phe ratio <0.1 indicates petroleum origins, while Ant/

Ant+Phe >0.1 indicates pyrogenic sources. Coal combustion sources can be recognized by a BaA/BaA+Chr ratio between 0.2 and 0.35, while BaA/BaA+Chr >0.35 suggests vehicular emission (Tobiszewski and Namiesnik 2012). An IcdP/Icdp+BghiP ratio <0.4 typically indicates petroleum origins, whereas IcdP/Icdp+BghiP >0.5 is suggestive of pyrogenic sources.

2.4 Statistical Analysis

Multivariate statistical analyses of the data were conducted using the SPSS v. 16.0. Duncan's range test was performed to demonstrate seasonal variations and spatial variations of different elements and total PAHs. $p < 0.01$ showed an extremely significant difference and $p < 0.05$ indicated a significant difference.

3 Results and Discussion

3.1 Atmospheric Deposition Rate

The daily average deposition rates at different sites in Shanghai are shown in Fig. 2. Throughout the year, the average deposition rates (DS) at all sites (183.3 ± 95.3, 121.5 ± 55.1, 109.9 ± 56.8, 115.0 ± 43.3, and 99.3 ± 46.3 mg/m^2/day from the city center outward) were higher than that of the background site (79.9 ± 32.1 mg/m^2/day). The highest average deposition rate was found at site 1 (the city center), which is in agreement with Cao et al. (2011), who reported that urban sites had higher
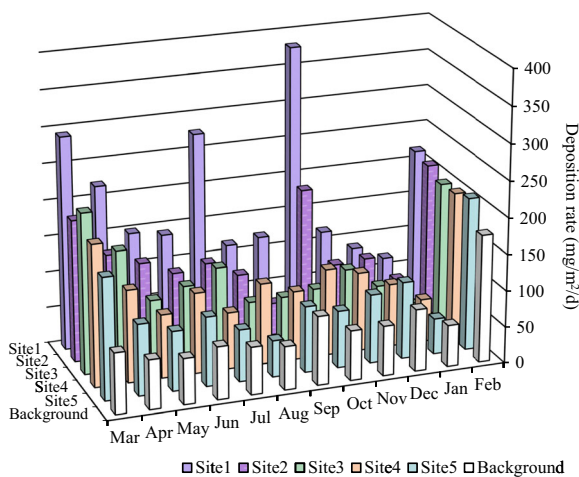
Fig. 2 Atmosphere deposition rate at different sites in Shanghai

average deposition rates than rural sites due to urban activities.

The seasonal variation of the atmospheric DS at the background site was minimal, with the exception of February. In China, the Spring Festival typically occurs in February, and fireworks and firecrackers, producing smoke and dust, are used in the celebrations. There was a similar pattern in seasonal variation at sites 2, 3, 4, and 5, with higher values in February, March, and April. Similar results were also reported in the Xi'an (Cao et al. 2011) and Guangzhou areas (Huang et al. 2014), where the deposition fluxes was at their maxima in spring, most likely a result of fuel combustion and vehicle emissions (Klumpp et al. 2003; Loppi et al. 2004). Generally, the prevailing wind in the spring in Shanghai was from the south or southeast of China, where there were larger emissions of dust from the increased consumption of coal in industrial production (Fig. 1), which played an important role in the higher atmospheric DS in the spring in Shanghai. Furthermore, even though the total rainfall in the spring is less than the total rainfall for the other seasons in Shanghai, there are many days with drizzle in the spring, which are conducive to wet deposition. In addition, the diffusion of deposition was abated, and the vertical transportation of particles was enhanced because of the weak wind in the spring.

There were significant differences at site 1, where the atmospheric DS displayed irregular patterns of seasonal variation, and the values observed in February (217.3 mg/m^2/day), March (293.3 mg/m^2/day), April (221.2 mg/m^2/day), July (277.1 mg/m^2/day), and October (381.4 mg/m^2/day) were relatively higher than the values for the other months. In addition to the rainfall and the wind force, the increased atmospheric DS might also be related to the location of site 1, which is in the commercial area (Fig. 1), and had a significant increase in population density and traffic volume, especially in October because of China's National Day. Similar results were also reported by Garban et al. (2002), who discovered that the bulk deposition fluxes were affected by local population density.

The annual average deposition rate for Shanghai was $43,100 \pm 54,800$ mg/m^2/year. Compared with results reported in the past 10 years, the deposition rate of Shanghai was 8.3 times higher than in Sapporo, Japan (Uematsu et al. 2003), 1.4 times higher than in Namoi Valley, Australia (Cattle et al. 2002), 0.6 times lower than in the Xi'an area (Cao et al. 2011), 0.3 times lower than in Beijing (Zhang et al. 2004), and 0.9 times lower

than in the German Alps (Kufmann 2006). In addition to the combustion of fossil fuels and heavy traffic, these results could be explained by their distance from the pollution sources.

3.2 Content, Sources, and Distribution of Metallic Element

3.2.1 The Effect of Spatial Distribution on Elemental Concentrations

The elemental contents in the atmospheric deposition samples collected from the sites are listed in Table 1. No variations were observed in the concentrations of Al, Ti, V, K, Na, and Mg among the different sites. These elements are among the chief materials found in the Earth's crust, and the parent material may be the dominant factor influencing the distribution of these elements in soils (Petrotou et al. 2012). Therefore, the distribution of these elements in deposited particles was unaffected by the location of the sampling sites (Shi et al. 2012). The concentrations of Cr, Mn, Co, Ni, Zn, Pb, and Cd did not display a regular pattern for the sampling sites; however, the highest concentration of Cu was observed at site 4, and the highest concentrations of the other elements were observed at site 5. At

these sites, the concentrations were significantly higher than the background, which was most likely due to nearby pollution sources (Liang et al. 2011). Because sites 5 and 4 were situated on the urban fringe, they may have been influenced by power generation facilities as well as chemical and coking plants. The highest concentrations of Cr, Mn, Co, Ni, Cu, Zn, Pb, and Cd were 604.1 ± 418.5, 935.7 ± 341.9, 15.5 ± 4.1, 124.3 ± 57.0, 931.2 ± 152.7, $1,149.4 \pm 563.1$, 328.3 ± 140.0, and 2.0 ± 0.9 mg/kg, respectively, which were one to ten times higher than those at the background site. Interestingly, although As is not a crustal element, its concentration did not vary much between the different sites with phenomenon similar to those of the crustal elements. Thus, further studies are needed to determine on these reasons.

Table 2 shows the elemental deposition rates for different sampling sites. The highest deposition rates of Mn, Co, Zn, Pb, and Cd were observed at Site 1, even though the contents of some elements (e.g., Zn, Pb, and Cd) in the samples collected at the site were low. The city center generally has higher traffic volume, which is likely to increase the dust deposition. In addition, compared to the suburbs and the background site, the urban area is a relatively closed space, which would prevent the diffusion of dust. The highest deposition

Table 1 Elemental contents of atmospheric deposition samples from different sites in Shanghai (milligrams per kilogram)

Elements	Sampling locations					
	Site 1	Site 2	Site 3	Site 4	Site 5	Reference-B
Ai*	40.4 ± 9.5^a	33.7 ± 6.6^a	37.2 ± 4.4^a	37.5 ± 4.5^a	41.7 ± 6.6^a	37.6 ± 10.9^a
Ti*	2.7 ± 0.5^a	3.2 ± 1.0^a	3.4 ± 0.9^a	2.9 ± 0.3^a	3.3 ± 0.7^a	3.4 ± 1.5^a
V	54.0 ± 7.7^a	66.2 ± 37.1^a	59.6 ± 10.3^a	59.2 ± 6.6^a	59.3 ± 7.8^a	46.8 ± 14.1^a
Cr	162.8 ± 59.8^b	279.8 ± 125.3^b	231.9 ± 80.0^b	195.6 ± 48.6^b	604.1 ± 418.5^a	173.1 ± 105.8^b
Mn	608.4 ± 117.6^b	871.9 ± 402.0^a	746.9 ± 132.0^a	591.7 ± 138.6^b	935.7 ± 341.9^a	381.3 ± 112.8^c
Co	9.4 ± 1.1^b	12.1 ± 4.3^b	10.5 ± 1.1^b	10.8 ± 1.1^b	15.5 ± 4.1^a	8.4 ± 2.0^c
Ni	48.6 ± 12.1^b	85.7 ± 33.5^b	68.9 ± 18.1^b	63.1 ± 11.4^b	124.3 ± 57.0^a	63.1 ± 46.8^b
Cu	290.6 ± 262.4^b	402.1 ± 322.3^b	249.0 ± 44.8^b	931.2 ± 152.7^a	272.4 ± 136.9^b	97.8 ± 44.7^b
Zn	726.4 ± 196.5^b	$1,021.2 \pm 424.1^a$	967.8 ± 329.9^a	719.9 ± 218.6^b	$1,149.4 \pm 563.1^a$	346.8 ± 125.1^c
As	29.0 ± 7.9^a	39.8 ± 18.5^a	33.9 ± 20.2^a	41.0 ± 16.9^a	32.5 ± 7.0^a	31.1 ± 8.7^a
Cd	1.9 ± 0.8^a	2.3 ± 0.9^a	2.1 ± 0.9^a	1.6 ± 1.0^a	2.0 ± 0.9^a	1.0 ± 0.4^b
Pb	232.1 ± 64.3^{ab}	335.9 ± 165.0^a	292.3 ± 65.5^a	280.8 ± 54.7^a	328.3 ± 140.0^a	163.5 ± 66.2^b
K*	14.1 ± 2.2^a	20.3 ± 22.7^a	14.4 ± 1.5^a	13.8 ± 1.3^a	15.0 ± 1.4^a	14.8 ± 2.4^a
Na*	8.7 ± 1.6^a	7.5 ± 1.3^a	7.8 ± 0.8^a	8.0 ± 1.1^a	8.0 ± 1.1^a	8.3 ± 2.4^a
Mg*	8.4 ± 1.6^a	8.0 ± 1.6^a	$9.0 \pm 1.1a$	7.8 ± 1.5^a	7.7 ± 2.1^a	7.1 ± 2.7^a

Note: *asterisk* indicates that the units are %, while the units of all other elements are milligrams per kilogram

Table 2 Deposition rates of elements for the atmospheric deposition samples from different sites in Shanghai (milligrams per square meter per day)

	Site 1	Site 2	Site 3	Site 4	Site 5	Background
AL	2581 ± 1152	1341 ± 699	1501 ± 860	1574 ± 638	1553 ± 881	971 ± 764
Ti	173 ± 76	126 ± 69	139 ± 94	122 ± 49	121 ± 68	72 ± 61
V	3.6 ± 2.0	2.4 ± 1.1	2.4 ± 1.5	2.5 ± 1.1	2.2 ± 1.3	1.2 ± 1.1
Cr	11 ± 6.8	10 ± 5.4	8.9 ± 4.9	8.0 ± 3.3	22 ± 19	3.4 ± 3.4
Mn	40 ± 22	31 ± 13	29 ± 14	24 ± 9.1	33 ± 18	9 ± 6.9
Co	0.62 ± 0.32	0.46 ± 0.19	0.41 ± 0.21	0.45 ± 0.16	0.55 ± 0.29	0.20 ± 0.17
Ni	3.2 ± 1.7	3.1 ± 1. 2	2.6 ± 1.2	2.6 ± 0.89	4.6 ± 3.4	1.1 ± 1.1
Cu	17 ± 9.1	14 ± 12	9.5 ± 4.0	330 ± 516	9.5 ± 6.6	2.5 ± 2.0
Zn	50 ± 32	38 ± 17	37 ± 19	29 ± 13	37 ± 16	7.9 ± 6.6
As	2.0 ± 1.3	1.4 ± 0.61	1.3 ± 0.78	1.8 ± 1.1	1.2 ± 0.72	0.8 ± 0.77
Cd	0.15 ± 0.13	0.10 ± 0.068	0.089 ± 0.071	0.070 ± 0.064	0.067 ± 0.032	0.023 ± 0.019
Pb	15 ± 8.9	13 ± 7.8	13 ± 9.2	12 ± 6.5	12 ± 7.9	4.0 ± 3.8
K	945 ± 499	661 ± 441	586 ± 332	587 ± 257	552 ± 288	379 ± 324
Na	679 ± 464	296 ± 441	315 ± 332	330 ± 257	292 ± 288	220 ± 324
Mg	575 ± 401	314 ± 166	358 ± 195	316 ± 103	274 ± 126	160 ± 121

rates of Cr and Ni were observed at site 5, and the highest deposition rate of Cu was observed at site 4. Figure 2 implied that the DS of these two sampling sites were relatively lower, and Table 1 showed that the samples from atmospheric deposition from sites 4 and 5 tended to have higher concentrations of Cu and higher concentrations of Cr and Ni, respectively, which led to the higher deposition of the elements. Ambient industrial districts might be the reason higher concentrations of Cu, Cr, and Ni existed in the samples.

The enrichment factor (EF) can be used to calculate the extent of the accumulation of elements in specific environments and can identify both anthropogenic interferences and specific sources of elements (Lu et al. 2009). The EFs of all elements are shown in Fig. 3. The EFs of Al, V, Co, K, Na, and Mg were <2, which indicated minimal influence of anthropogenic activities on these elements. Elements with an EF between 2 and 5 included Cr, Ni, As, and Mo, and these elements were considered to be moderately enriched in the deposition samples. At sites 4 and 5, which were situated in urban-rural zones with some factories, the EFs of As, Cr, and Mo exceeded 5. Therefore, the presence of these elements in the deposition samples was influenced by the industries present, and several recent studies also obtained the same results (Sandroni and Migon 2002; Mijic et al. 2010; Okubo et al. 2013; Kara et al. 2014). For Cu, Zn, Cd, and Pb, the EFs normally ranged from 5 to 20; in fact, in certain samples, the EF of Cu was greater than 20, implying significant enrichment. These elements were also found to have a higher atmospheric deposition rate than the other elements, which may be related to anthropogenic inputs (e.g., traffic and construction). Generally, Cu and Pb are emitted from fossil fuel combustion, the abrasion of tires and brake linings, and the corrosion of galvanized protection barriers (Dierkes and Geiger 1999; Fakayode and Olu-Owolabi 2003; Fang et al. 2009). Zinc is also a marker for brake lining wear and is a metal widely used in building materials and automotive components (Liu et al. 1996). Cadmium originates from electroplating and batteries. Although unleaded gasoline has been used in Shanghai since October 1, 1997 (Fang et al. 2009), the EF of Pb was still very high. This heavy metal deposition behavior was also reported by Gunawardena et al. (2013), who concluded that reducing traffic congestion would be more effective than reducing traffic volume for improving air quality, particularly in relation to Pb, Cd, Zn, and Cu.

### 3.2.2 The Effect of Seasonal Variation on Elemental Concentrations

To clearly represent the seasonal variation of elemental concentrations, deposition rates of all elements were standardized by using the min–max normalization and
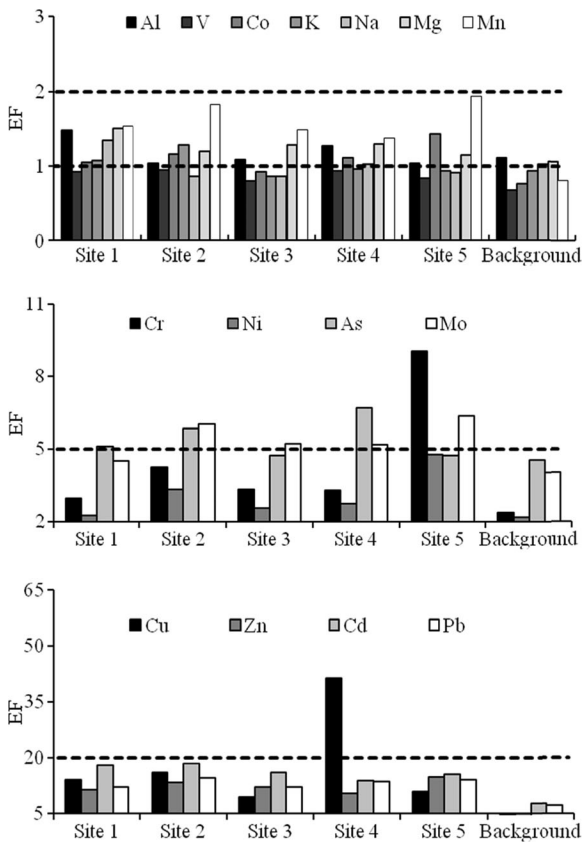
Fig. 3 Enrichment factors of the elements in the atmospheric deposition samples at different sites in Shanghai

standardized deposition rates of all elements over a 12-month period are displayed in Fig. 4. The Al, Ti, V, Co, K, Na, Mg, Cr, Ni, Mn, and Pb depositional fluxes were higher in February and March than in any other months. The fireworks are primarily composed of explosives (charcoal, sulfur, and potassium nitrate) and mud, and other elements (such as Na, Mg, Cr, and Ni) are added to provide the colors. Therefore, the deposition rates of Na, Mg, Cr, and Ni were much higher in February. Moreover, fireworks might also cause the splashing of dust on the ground, which would likely lead to increased Al and Ti deposition rates, although no significant seasonal trend for Al and Ti, which were generally characterized as crustal elements (Azimi et al. 2005), was observed (Fig. 4s). In addition, higher depositional fluxes for these elements might be related to the higher dust deposition rate in March (Fig. 1). However, higher depositional flux for Cu was found from June to September, which might be attributed to the seasonal trend for Cu concentrations (Fig. 4s). Higher Zn and Cd concentrations were also found in March, April, July, and October, which indicated that their
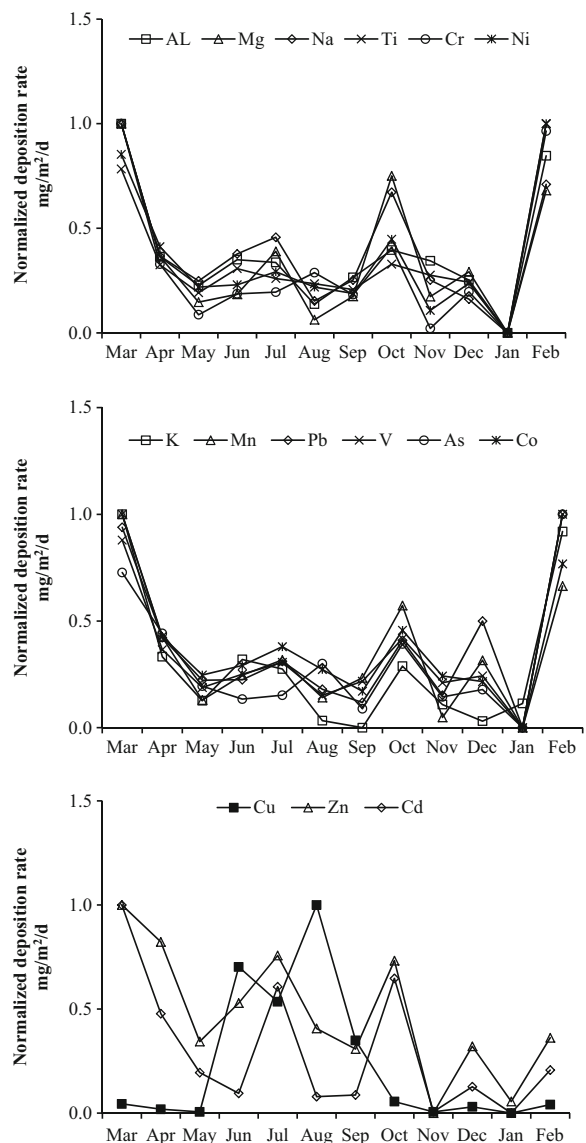
Fig. 4 The min-max normalized deposition rate of elements from atmospheric deposition samples collected in different months

distribution may be related to emissions of coarse particles as a result of fuel combustion. Many studies indicated that automotive exhaust emissions and tire friction would easily lead to Cd and Zn pollution, but no significant seasonal variation for Pb was observed during the year, which might be because of the use of unleaded gasoline in Shanghai since October 1997 (Fang et al. 2009). Moreover, heavy rainfall most likely led to the relatively high elemental concentrations, as wet deposition during rainfall makes a large contribution to the total atmospheric deposition (Hustona et al. 2009). This was one of main reasons for

the differences between the results of this and other studies where only dry atmospheric deposition was monitored (Zhang et al. 2004; Sabin et al. 2006; Shi et al. 2012).

3.3 Content and Distribution of PAHs

3.3.1 The Effect of Spatial Location on PAH Concentrations

All 16 PAHs were detected in the atmospheric deposition samples, and the total PAHs measured at the different sites are presented in Fig. 5. The mean concentrations of the PAHs were in the following order: site 5 (14.81 $\pm$ 1.05 mg/kg) $\approx$ site 4 (14.17 $\pm$ 1.30 mg/kg) > site 3 (12.02 $\pm$ 0.50 mg/kg) > site 2 (10.49 $\pm$ 0.87 mg/kg) > site 1 (5.57 $\pm$ 1.20 mg/kg) > background (4.76 $\pm$ 0.78 mg/kg). There were significant differences between the different sites ($p < 0.01$), which was consistent with results published previously by Garban et al. (2002), who determined that the lowest PAH depositions were found in rural and forested sites. The PAH concentrations in Shanghai were lower than in the Beijing–Tianjin region, where the concentrations of PAHs varied from 4.22 to 24.81 mg/kg (mean = 11.81 mg/kg; Wang et al. 2011). This may be a consequence of the large amount of coal and biofuel burned for residential heating as well as higher traffic flow. Similar to the concentration of PAHs, the deposition fluxes of the PAHs also followed this order: the urban fringe zone (sites 5, 4, and 3) > the city center (sites 1 and 2) > the rural zone (background site). The deposition fluxes of the PAHs ranged from 0.38 to 1.63 mg/m^2/day (mean = 1.19 $\pm$ 0.45 mg/m^2/day), which were higher than those in Paris (France; Garban et al. 2002), western Greece (Terzi and Samara 2005), the Pyrenees, the Alps, and the Caledonian mountains (Fernández et al. 2003), and the Nature Park of Spain (Foan et al. 2012), but lower than those in Tampa
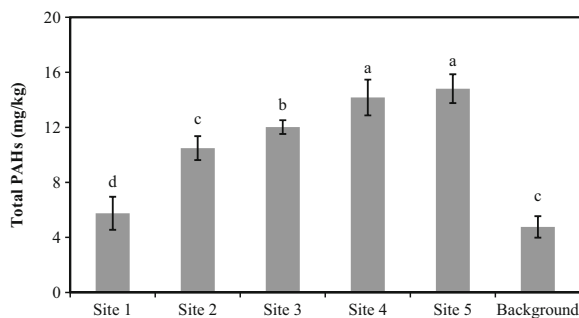

Fig. 5 The total PAH content of atmospheric deposition samples at different sites in Shanghai

Bay (USA; Poor et al. 2004), Manchester and Cardiff (UK) (Halsall et al. 1997), and the industrial district of Bursa, Turkey (Esen et al. 2008).

3.3.2 The Effect of Seasonal Variation on PAH Concentrations

The depositional fluxes of the PAHs over the months tested are plotted in Fig. 6 and were defined by the product of the deposition rate and the PAH concentration. There were higher PAH depositional fluxes in March, July, and October, which was consistent with the deposition rate described in Fig. 2. PAH depositional fluxes are primarily influenced by emissions, compound properties, atmospheric conditions and meteorological factors. The high PAH concentrations were most likely due to high vehicular traffic volume, a large number of factories, and the dense population in the Shanghai region (Yan et al., 2012). Because the cold air is more active in winter in Shanghai, the diffusion of pollutants is easily accelerated by strong winds, which leads to smaller PAH depositional fluxes. The lower horizontal wind speed and stronger vertical atmospheric convection in summer are unfavorable to the diffusion of particles but enhance their vertical transportation and consequently lead to higher PAH depositional fluxes (Cheng et al. 2015). Higher PAH depositional flux in October is most likely due to the increased population density and traffic volume associated with Chinese National Day. In light of lower temperatures and weak winds in March, higher PAH depositional fluxes were most likely due to increased fuel combustion for heating. A previous study concluded that rainfall and temperature were crucial factors in controlling the behavior of PAHs because they influenced the partitioning between the gas and particle phases. However, there was no significant correlation between the PAH depositional fluxes and rainfall or temperature in this study, which differed from the results obtained in Hong Kong (Liu et al. 2013). This probably contributed to the differences in the abundance of individual PAH compounds. Low-molecular-weight (LMW) PAHs (the two- to three-ring PAHs) were found predominantly in the gas phase, whereas the high-molecular-weight (HMW) PAHs (four- to six-ring PAHs) were typically associated with airborne particles (Gundel et al. 1995; Lighty et al. 2000). Furthermore, the effects of rainfall and temperature on the gas phase were much greater than they were on the particulate phase (Teil et al. 2004; Li et al. 2009).
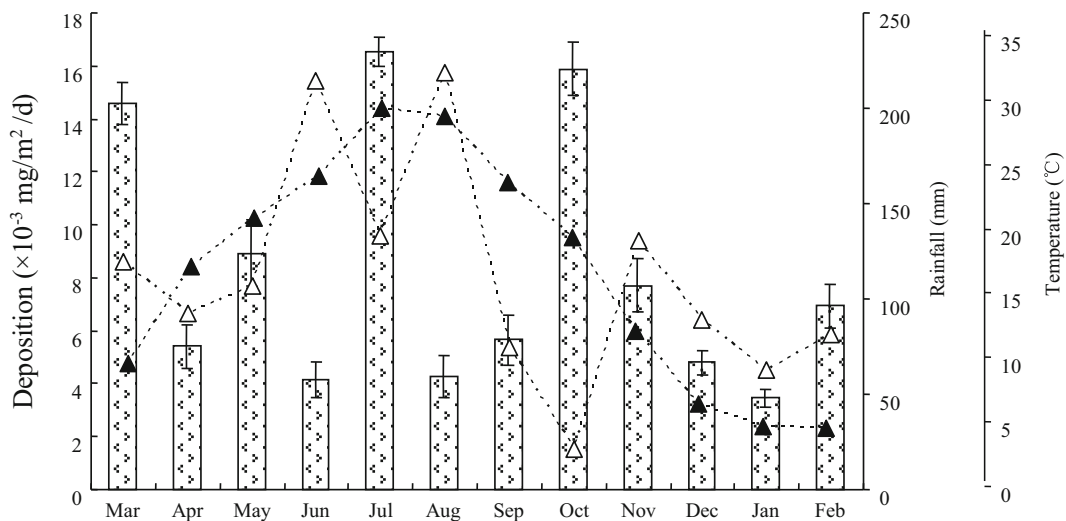
Fig. 6 Seasonal variations of PAH deposition fluxes, temperature, and rainfall.

Furthermore, the LMW PAHs accounted for 63 % of the total PAHs in the dry season (from October to March) and 52 % in the wet season (from April to September) in Hong Kong, while the LMW PAHs accounted for a maximum of only 31.1 % in this study.

3.3.3 Source Analysis of PAHs

The Ant/Ant+Phe, BaA/BaA+Chr, and IcdP/Icdp+ BghiP ratios in the atmospheric deposition samples collected from the different sites are listed in Table 3. In this study, the Ant/Ant+Phe ratio was approximately 0.1 and ranged from 0.073 to 0.18. Therefore, the sources of the PAHs in the atmospheric deposition samples were predominantly petroleum and fossil fuel combustion. The IcdP/Icdp+BghiP ratio was close to 0.5, which indicated petroleum, grass, wood, and coal combustion. However, the BaA/BaA+Chr ratio was higher than 0.35, which implied the possible influence of vehicular emission. In addition, a BaA/BaA+Chr ratio

>0.4 was found at the background site, which indicated that these sites were most likely influenced by urban PAHs emission (Mantis et al. 2005; Tobiszewski and Namiesnik 2012). These results concur with those regarding the rainwater in Shanghai (Yan et al. 2012). The LMW PAHs were predominantly derived from the incomplete combustion of petroleum, while the HMW PAHs were mostly associated with other combustion sources (Chen et al. 2005; Wilcke 2007).

4 Conclusions

The average deposition rates (DS) at five sites were higher than those at the background site throughout the year, and the highest average DS was found at site 1. The atmospheric DS at all sites were higher in February, March, April, July, and October. There was a significant increase in enrichment of Cu, Zn, Cd, and Pb. Higher depositional fluxes of Zn, Pb, and Cd were

Table 3 Diagnostic values of selected PAHs for the atmospheric deposition samples at different sites (Tobiszewski and Namiesnik 2012)

	Site 1	Site 2	Site 3	Site 4	Site 5	Background	Source identification	
IcdP/(Icdp+BghiP)	0.52	0.52	0.51	0.51	0.52	0.52	<0.4	Petroleum
							>0.5	Combustion
Ant/(Ant+Phe)	0.18	0.073	0.14	0.18	0.14	0.11	<0.1	Petroleum
							>0.1	Combustion
BaA/(BaA+Chr)	0.35	0.40	0.40	0.44	0.48	0.46	0.2–0.35	Coal combustion
							>0.35	Vehicular emissions

observed at site 1, and higher depositional fluxes Cu were observed at site 4. The deposition fluxes of the PAHs exhibited the following order: urban fringe zone (sites 5, 4, and 3) > city center (sites 1 and 2) > rural zone (background site). Higher PAH depositional fluxes were observed in March, July, and October. According to the ratios of the individual PAH species, petroleum and combustion were the main PAH sources, but the use of coal ovens may be another factor influencing the distribution of PAHs in the suburbs.

References

Abrahams, P. W. (2002). Soils: their implications to human health. *Science of the Total Environment, 291*, 1–32.

Amodio, M., Catino, S., Dambruoso, P. R., de Gennaro, G., Di Gilio, A., Giungato, P., Laiola, E., Marzocca, A., Mazzone, A., Sardaro, A., & Tutino, M. (2014). *Advances in Meteorology*. http://dx.doi.org/10.1155/2014/161730.

Azimi, S., Ludwig, A., Thevenot, D. R., Colin, J. L. (2003). Trace metal determination in total atmospheric deposition in rural and urban areas. *Science of the Total Environment, 308*, 247–254.

Azimi, S., Rocher, V., Muller, M., Moilleron, R., & Thevenot, D. R. (2005). Sources, distribution and variability of hydrocarbons and metals in atmospheric deposition in an urban area (Paris, France). *Science of the Total Environment, 337*, 223–239.

Bari, M. A., Kindzierski, W. B., & Cho, S. (2014). A wintertime investigation of atmospheric deposition of metals and polycyclic aromatic hydrocarbons in the Athabasca Oil Sands Region, Canada. *Science of the Total Environment, 485–486*, 180–192.

Cao, Z. Z., Yang, Y. H., Lu, J. L., & Zhang, C. X. (2011). Atmospheric particle characterization, distribution, and deposition in Xi'an, Shaanxi Province, Central China. *Environmental Pollution, 159*, 577–584.

Cattle, S. R., McTainsh, G. H., & Wagner, S. (2002). Aeolian dust contributions to soil of the Namoi Valley, Northern NSW, Australia. *Catena, 47*, 245–264.

Chen, J., Wei, F., Zheng, C., Wu, Y., & Adriano, D. C. (1991). Background concentrations of elements in soils of China. *Water, Air, and Soil Pollution, 57–58*, 699–712.

Chen, L., Ran, Y., Xing, B., Mai, B., He, J., Wei, X., Fu, J., & Sheng, G. (2005). Contents and sources of polycyclic aromatic hydrocarbons and organochlorine pesticides in vegetable soils of Guangzhou, China. *Chemosphere, 60*, 879–890.

Cheng, T.T., Xu, C., Duan, J.Y., Wang, Y.F., Leng, C.P., Tao, J., Che, H.Z., He, Q.S., Wu, Y.F., Zhang, R.J., Li, X., Chen, J.M., Kong, L.D., Y, X.N., (2015). Seasonal variation and difference of aerosol optical properties in columnar and surface atmospheres over Shanghai. *Atmospheric Environment, in press*, 1-12.

Davis, B. L., & Guo, J. (2000). Airborne particulate study in five cities of China. *Atmospheric Environment, 34*, 2703–2711.

Dierkes, C., & Geiger, W. F. (1999). Pollution retention capabilities of roadside soils. *Water Science Technology, 39*, 201–208.

Esen, F., SiddIk Cindoruk, S., & Tasdemir, Y. (2008). Bulk deposition of polycyclic aromatic hydrocarbons (PAHs) in an industrial site of Turkey. *Environmental Pollution, 152*, 461–467.

Fakayode, S. O., & Olu-Owolabi, B. (2003). Heavy metal contamination of roadside topsoil in Osogbo, Nigeria: its relationship to traffic density and proximity to highways. *Environmental Geology, 44*, 150–157.

Fang, H. L., Dong, Y., Gu, B., Hao, G. J., Lv, Z. W., Liang, J., & Chen, L. (2009). Distribution of heavy metals and arsenic in greenbelt roadside soils of Pudong new district in Shanghai. *Soil and Sediment Contamination, 18*, 702–714.

Feng, J. L., Li, M., Zhang, P., Gong, S. Y., Zhong, M., Wu, M. H., Zheng, M., Chen, C. H., Wang, H. L., & Lou, S. R. (2013). Investigation of the sources and seasonal variations of secondary organic aerosols in PM2.5 in Shanghai with organic tracers. *Atmospheric Environment, 79*, 614–622.

Fernández, P., Carrera, G., Grimalt, J. O., Ventura, M., Camarero, L., Catalan, J., Nickus, U., Thies, H., & Psenner, R. (2003). Factors governing the atmospheric deposition of polycyclic aromatic hydrocarbons to remote areas. *Environmental Science & Technology, 37*, 3261–3267.

Foan, L., Domerq, M., Bermejo, R., Santamaria, J. M., & Simon, V. (2012). Polycyclic aromatic hydrocarbons (PAHs) in remote bulk and throughfall deposition: seasonal and spatial trends. *Engineering and Management Journal, 11*, 1101–1110.

Garban, B., Blanchoud, H., Motelay-Massei, A., Chevreuil, M., & Ollivon, D. (2002). Atmospheric bulk deposition of PAHs onto France: trends from urban to remote sites. *Atmospheric Environment, 36*, 5395–5403.

GB/T 15265-1994. Ambient air-determination of dustfall-gravimetric method (in Chinese).

Golomb, D., Ryan, D., Eby, N., Underhill, J., & Zemba, S. (1997). Atmospheric deposition of toxic onto Massachusetts Bay - I. Metals. *Atmospheric Environment, 31*, 1349–1359.

Gunawardena, J., Egodawatta, P., Ayoko, G. A., & Goonetilleke, A. (2013). Atmospheric deposition as a source of heavy metals in urban stormwater. *Atmospheric Environment, 68*, 235–242.

Gundel, L. A., Lee, V. C., Mahanama, K. R. R., Stevens, R. K., & Daisey, J. M. (1995). Direct determination of the phase distribution of semi-volatile polycyclic aromatic hydrocarbons using annular denuders. *Atmospheric Environment, 29*, 1719–1733.

Halsall, C. J., Coleman, P. J., & Jones, K. C. (1997). Atmospheric deposition of polychlorinated dibenzo-p-dioxins/dibenzofurans (PCDD/Fs) and polycyclic aromatic hydrocarbons (PAHs) in two UK cities. *Chemosphere, 35*, 1919–1931.

Huang, W., Duan, D. D., Zhang, Y. L., Cheng, H. F., & Ran, Y. (2014). Heavy metals in particulate and colloidal matter from atmospheric deposition of urban Guangzhou, South China. *Marine Pollution Bulletin, 85*, 720–726.

Hustona, R., Chana, Y. C., Gardnerc, T., Shawe, G., & Chapman, H. (2009). Characterisation of atmospheric deposition as a

source of contaminants in urban rainwater tanks. *Water Research, 43*, 1630–1640.

Kara, M., Dumanoğlu, Y., Altıok, H., Elbir, T., Odabası, M., & Bayram, A. (2014). Seasonal and spatial variation of atmospheric trace elemental deposition in the Aliaga industrial region, Turkey. *Atmospheric Research, 149*, 204–216.

Klumpp, A., Hintemann, T., Santana, Lima, J., & Kandeler, E. (2003). Bioindication of air pollution effects near a copper smelter in Brazil using mango trees and soil microbiological properties. *Environmental Pollution, 126*, 313–321.

Kufmann, C. (2006). Measurement and climatic control of eolian sedimentation on snow cover surface in the northern Calcareous Alps (Wetterstein-Karwendel and Berchtesgadener Alps, Germany). *Zeitschrift Fur Geomorphologie, 50*, 245–268.

Lee, M. L., Novotny, M., & Bartle, K. D. (1981). *Analytical Chemistry of Polycyclic Aromatic Compounds*. New York: Academic Press.

Liang, J., Ma, G. J., Fang, H. L., Chen, L., & Christiw, P. (2011). Polycyclic aromatic hydrocarbon concentrations in urban soils representing different land use categories in Shanghai. *Environmental Earth Sciences, 62*, 33–42.

Li, J., Cheng, H., Zhang, G., Qi, S. H., & Li, X. D. (2009). Polycyclic aromatic hydrocarbon (PAH) deposition to and exchange at the air-water interface of Luhu, an urban lake in Guangzhou, China. *Environmental Pollution, 157*, 273–279.

Lighty, J. S., Veranth, J. M., & Sarom, A. F. (2000). Combustion aerosols: factors governing their size and composition and implications to human health. *Journal of the Air & Waste Management Association, 50*, 1565–618.

Liu, Y. L., Takamatsu, T., & Sase, H. (1996). Study on soil pollution with heavy metal in some Japanese cities. *Research Environmental Sciences, 9*, 47–51 (in Chinese).

Liu, F. B., Xu, Y., Liu, J. W., Liu, D., Li, J., Zhang, G., Li, X. D., Zou, S. C., & Lai, S. C. (2013). Atmospheric deposition of polycyclic aromatic hydrocarbons (PAHs) to a coastal site of Hong Kong, South China. *Atmospheric Environment, 69*, 265–272.

Loppi, S., Frati, L., Paoli, L., Bigagli, V., Rossetti, C., Bruscoli, C., & Corsini, A. (2004). Biodiversity of epiphytic lichens and heavy metal contents of Flavoparmelia caperata thalli as indicators of temporal variations of air pollution in the town of Montecatini Terme (central Italy). *Science of the Total Environment, 326*, 113–122.

Lu, X., Li, L. Y., Wang, L., Lei, K., Huang, J., & Zhai, Y. (2009). Contamination assessment of mercury and arsenic in roadway dust from Baoji, China. *Atmospheric Environment, 43*, 2489–2496.

Mantis, J., Chaloulakou, A., & Samara, C. (2005). PM10-bound polycyclic aromatic hydrocarbons (PAHs) in the Greater Area of Athens, Greece. *Chemosphere, 59*, 593–604.

Martín, J., Sanchez-Cabeza, J., Eriksson, M., Levy, I., & Miquel, J. C. (2009). Recent accumulation of trace metals in sediments at the DYFAMED site (Northwestern Mediterranean Sea). *Marine Pollution Bulletin, 59*, 146–153.

Mijic, Z., Stojic, A., Perisic, M., Rajsic, S., Tasic, M., Radenkovic, M., & Joksic, J. (2010). Seasonal variability and source apportionment of metals in the atmospheric deposition in Belgrade. *Atmospheric Environment, 44*, 3630–3637.

Okubo, A., Takeda, S., & Obata, H. (2013). Atmospheric deposition of trace metals to the western North Pacific Ocean observed at

coastal station in Japan. *Atmospheric Research, 129–130*, 20–32.

Poor, N., Tremblay, R., Kay, H., Bhethanabotla, V., Swartz, E., Luther, M., & Campbell, S. (2004). Atmospheric concentrations and dry deposition rates of polycyclic aromatic hydrocarbons (PAHs) for Tampa Bay, Florida, USA. *Atmospheric Environment, 38*, 6005–6015.

Peng, C., Ouyang, Z. Y., Wang, M. I., Chen, W. P., & Jiao, W. T. (2012). Vegetative cover and PAHs accumulation in soils of urban green space. *Environmental Pollution, 161*, 36–42.

Petrotou, A., Skordas, K., Papastergios, G., Filippidis, A. (2012). Factors affecting the distribution of potentially toxic elements in surface soils around an industrialized area of northwestern Greece. *Environ Earth Science, 65*, 823–833.

Ravindra, K., Sokhi, R., & Van Grieken, R. (2008). Atmospheric polycyclic aromatic hydrocarbons: Source attribution, emission factors and regulation. *Atmospheric Environment, 42*, 2895–2921.

Sabin, L. D., Lim, J. H., Venezia, M. T., Winer, A. M., Schiff, K. C., & Stolzenbach, K. D. (2006). Dry deposition and resuspension of particle-associated metals near a freeway in Los Angeles. *Atmospheric Environment, 40*, 7528–7538.

Sandroni, V., & Migon, C. (2002). Atmospheric deposition of metallic pollutants over the Ligurian Sea: labile and residual inputs. *Chemosphere, 47*, 753–764.

Shanghai Municipal Statistics Bureau. (2010). *Shanghai statistical yearbook*. Beijing: China Statistics Press.

Shi, G., Chen, Z., Teng, J., Bi, C., Zhou, D., Sun, C., Li, Y., & Xu, S. (2012). Fluxes, variability and sources of cadmium, lead, arsenic and mercury in dry atmospheric depositions in urban, suburban and rural areas. *Environmental Research, 113*, 28–32.

Sutherland, R. (2000). Bed sediment-associated trace metals in an urban stream, Oahu, Hawaii. *Environmental Geology, 39*, 611–627.

Tasdemir, Y., & Esen, F. (2007). Urban air PAHs: Concentrations, temporal changes and gas/particle partitioning at a traffic site in Turkey. *Atmospheric Resource, 84*, 1–12.

Teil, M. J., Blanchard, M., & Chevreuil, M. (2004). Atmospheric deposition of organochlorines (PCBs and pesticides) in northern France. *Chemosphere, 55*, 501–514.

Terzi, E., & Samara, C. (2005). Dry deposition of polycyclic aromatic hydrocarbons in urban and rural sites of Western Greece. *Atmospheric Environment, 39*, 6261–6270.

Tobiszewski, M., & Namiesnik, J. (2012). PAH diagnostic ratios for the identification of pollution emission sources. *Environmental Pollution, 162*, 110–119.

Uematsu, M., Wang, Z., & Uno, I. (2003). Atmospheric input of mineral dust to the western North Pacific region based on direct measurements and a regional chemical transport model. *Geophysical Research Letters, 30*, 1342.

Wang, W., Massey, Simonich, S. L., Giri, B., Xue, M., Zhao, J., Chen, S., Shen, H., Shen, G., Wang, R., Cao, J., & Tao, S. (2011). Spatial distribution and seasonal variation of atmospheric bulk deposition of polycyclic aromatic hydrocarbons in Beijing - Tianjin region, North China. *Environmental Pollution, 159*, 287–293.

Wilcke, W. (2007). Global patterns of polycyclic aromatic hydrocarbons (PAHs) in soil. *Geodema, 141*, 157–166.

Williams, P. T. (1990). Sampling and analysis of polycyclic aromatic compounds from combustion systems. A review. *Journal of the Energy Institute, 63*, 22–30.

Yan, L. L., Li, X., Chen, J. M., Wang, X. J., Du, J. F., & Ma, L. (2012). Source and deposition of polycyclic aromatic hydrocarbons to Shanghai, China. *Journal of Environmental Sciences, 24*, 116–123.

Yunker, M. B., Macdonald, R. W., Vingarzan, R., Mitchelld, R. H., Goyettee, D., & Sylvestrec, S. (2002). PAHs in the Fraser River basin: a critical appraisal of PAH ratios as indicators of PAH source and composition. *Organic Geochemistry, 33*, 489–515.

Zhang, R., Wang, M., Sheng, L., Kanai, Y., & Ohta, A. (2004). Seasonal characterization of dust days, mass concentration and dry deposition of atmospheric aerosols over Qingdao, China. *China Particuology, 2*, 196–199.

Zhang, H., Zhu, Y., Li, F., & Chen, L. (2011). Nutrients in the wet deposition of Shanghai and ecological impacts. *Physics and Chemistry of the Earth, 36*, 407–410.

Zhao, M. F., Huang, Z. S., Qiao, T., Zhang, Y. K., Xiu, G. L., & Yu, J. Z. (2015). Chemical characterization, the transport pathways and potential sources of $PM_{2.5}$ in Shanghai: Seasonal variations. *Atmospheric Research, 158–159*, 66–78.